Ross Barnowski, originally from Barrington, IL, is a junior at the University of Michigan majoring in Nuclear Engineering, Radiological Science and Engineering Physics. In the summer of 2008, he worked through the SULI program on remote detection of radioactive plumes using millimeter wave technology at Argonne National Laboratory. He is currently involved in research at the University of Michigan involving coupling real-time images with position-sensitive photon detection data. Ross also serves as the outreach chair for the Michigan student chapter of the American Nuclear Society. He will finish his B.S. degree in 2009 and hopes to pursue a Ph.D. in Nuclear Engineering. In his free time, he enjoys writing and playing music as the drummer in several local bands.

Hual-Te Chien received his Ph.D. degree in aerospace engineering and engineering mechanics from the University of Cincinnati in 1991. After his graduation, he joined the Sensor, Instrumentation and Nondestructive Evaluation section of the Energy Technology Division, Argonne National Laboratory. Dr. Chien has 22 years of experience in the area of sensors and instrumentation, nondestructive evaluation and testing (NDE/T), acoustics and vibration, data and image processing, experimental stress analysis and smart/intelligent materials and structures development. He has been developing ultrasonic spectroscope technique for material evaluation. Recently, he has developed microwave, millimeter and Terahertz spectroscope techniques for remote sensing and monitoring of bio-agents, chemicals and explosives, including a photoacoustic technique for remote detection. He has an extensive background in computer-aided design and analysis (CAD/CAA) and finite element analysis (FEA) of structures and systems. He has been author or co-author of more than 45 publications on the analytical study of wave propagation in solids, NDE of materials, sensors and instrumentation, smart materials and vibration control. Dr. Chien shared a 1994 R&D 100 Award for the invention of ultrasonic viscometer and an Argonne's Pacesetter Award for excellence in achievement and performance in 1997. He has been awarded seven U.S. patents and published more than 50 articles.

Nachappa "Sami" Gopalsami received his B.E. and M.S. degrees in Electrical Engineering from the University of Madras, India and his Ph.D. degree in Electrical Engineering and Computer Science from the University of Illinois, Chicago. He joined Argonne National Laboratory in 1980 where he is currently a Senior Electrical Engineer in the Sensors and Instrumentation section of the Nuclear Engineering Division. His current research interests include development of radio frequency, microwave, millimeter-wave and terahertz sensors and imaging systems for national security, biosensing, environmental monitoring and materials applications. Dr. Gopalsami has published over 150 technical papers in the area of sensors and nondestructive evaluation and has five U.S. patents to his credit. He has received two R&D 100 awards from R&D Magazine*, both on millimeter wave sensors in 1986 and 2007; an outstanding paper award from the American Society of Nondestructive Testing; and an Outstanding Mentor award from the Office of Science Undergraduate Research Programs. He is a senior member of IEEE and a member of Sigma Xi and SPIE.*

Remote Detection of Radioactive Plumes Using Millimeter Wave Technology

Ross Barnowski, Hual-Te Chien and Nachappa Gopalsami

ABSTRACT

The reprocessing of spent nuclear fuel, a common method for manufacturing weapons-grade special nuclear materials, is accompanied by the release of fission products trapped within the fuel. One of these fission products is a radioactive isotope of Krypton (Kr-85); a pure β^- emitter with a half-life of 10.72 years. Due to its chemical neutrality and relatively long half life, nearly all of the Kr-85 is released into the surrounding air during reprocessing, resulting in a concentration of Kr-85 near the source that is several orders of magnitude higher than the typical background (atmospheric) concentrations. This high concentration of Kr-85 is accompanied by a proportionately high increase in air ionization due to the release of beta radiation from Kr-85 decay. Millimeter wave (MMW) sensing technology can be used to detect the presence of Kr-85 induced plumes since a high concentration of ions in the air increases the radar cross section due to a combination of atmospheric phenomena. Possible applications for this technology include the remote sensing of reprocessing activities across national borders bolstering global anti-proliferation initiatives. The feasibility of using MMW radar technology to uniquely detect the presence of Kr-85 can be tested using commercial ion generators or sealed radioactive sources in the laboratory. In this paper we describe our work to derive an ion dispersion model that will describe the spatial distribution of ions from Kr-85 and other common lab sources. The types and energies of radiation emitted by isotopes Co-60 and Cs-137 were researched, and these parameters were incorporated into these dispersion models. Our results can be compared with the results of MMW detection experiments in order to quantify the relationship between radar cross section and air ionization as well as to further calibrate the MMW detection equipment.

Introduction

With the incredible potential for destruction attributed to nuclear weapons, the proliferation of special nuclear materials (SNM) is a notable concern for both national and global security. One possible method by which SNMs can be manufactured is the reprocessing of spent nuclear fuel. In fact, some reactors are designed specifically to enhance plutonium production for the purpose of bolstering nuclear weapons programs [1]. When nuclear fuel is reprocessed, fission products trapped within the fuel are released. One of the most prominent gaseous fission products is Krypton-85 (Kr-85), which is created in abundance in typical fission reactions. Kr-85 has a half-life of over 10 years, so it will not decay during the 1–2 year fuel-storage period that is typical before reprocessing occurs. Additionally, since Krypton is a noble-gas, it does not readily chemically react making it very difficult to suppress emissions of the gas during the reprocessing procedure [2]. Furthermore, Kr-85 is radioactive; a pure β^- emitter with an average energy of 251 keV/particle [3]. Studies have shown [4] that emissions of Kr-85 during reprocessing exceed the background (atmospheric) concentrations of the isotope by several orders of magnitude. Therefore, detection of Kr-85 offers a pragmatic and unique method for detecting the reprocessing of nuclear fuel.

Currently, the only way to detect the presence of Kr-85 is via atmospheric sampling [4]. Although effective under certain circumstances, this method has several drawbacks. First, collection efficiency is greatly affected by uncontrollable parameters such as wind, rough terrain and national borders. Wind and terrain can dramatically affect where and how far the plume of radioactive Kr-85 will spread. Furthermore, the detection efficiency decreases as distance from the source increases, so national borders impose a significant hurdle to international Kr-85 detection for nuclear fuel reprocessing plants far from borderlines. Additionally, it is neither practical nor cost-effective to continually sample the atmosphere, which limits the atmospheric collection method to applications where the time-frame of Kr-85 emissions is known. Ideally the disadvantages of the atmospheric collection method can be eliminated by using MMW radar to detect Kr-85 emissions directly near the source (the stack of a reprocessing plant).

The ability to cheaply and continuously monitor the output of known and suspected reprocessing facilities will greatly enhance the ability of international organizations to monitor compliance with non-proliferation treaties and initiatives. Rather than detect Kr-85 directly, the MMW radar will detect the ionized air that results from the emission of radioactive Kr-85. Ionized air has a higher radar cross-section than normal air, which allows plumes of radioactive gasses to be distinctly imaged or detected. Furthermore, other atmospheric phenomena such as ion-induced nucleation can further increase the radar cross-section of such plumes. These "tell tale" signatures in combination with the a priori knowledge of the plant and weather conditions would then indicate the presence of Kr-85, uniquely proving that fuel was being reprocessed. The goal of this project is to develop models for the spatial dispersion of ions, which can be used as a benchmark to test and calibrate the MMW system.

Centimeter-wave technology has been previously used to image the emissions of several commercial power plants [5]. However, the physical process by which radar cross section is increased due to radiation-induced ion concentration is complicated and, currently, not well understood. In the absence of a model that predicts radar cross section based on air ion concentration, experiments must be designed to test the response of the MMW technology to different sources and concentrations of ions. Therefore, it is important to derive models to predict the spatial distribution and concentration of ions from different sources so that the results of the experiments can be benchmarked.

Materials and Methods

Isotopes of Interest

The release and decay of Kr-85 is the most significant contributor to the increase in air ion concentration [2] during a reprocessing event. In fact, calculations using data from a study on reprocessing has shown that the ion concentration due to Kr-85 decay is expected to be three or more orders of magnitude greater than the atmospheric ion concentration [4]. However, Kr-85 is not an easily obtainable source for use in the laboratory due to the fact that its gaseous nature presents a significant health risk to laboratory personnel. Alternate sources such as Co-60 and Cs-137 are available from many vendors in the form of sealed disk sources, making them convenient for laboratory use. Although the types and energies of the radiation emitted from each of these sources differ from Kr-85, these sources are useful to study the MMW interaction of air ionization that occurs and the spatial distribution of those ions.

There are several parameters of interest in the construction of a spatially-dependent ion model, such as the path length of a typical beta particle (with given energy); the average number of ion pairs formed per energy of a beta particle; and contributions from gamma radiation. All of these parameters have a distinct affect on the derivation of a spatial ion model, and need to be taken into account for each of the individual isotopes. The energy spectra and decay modes of Kr-85, Co-60 and Cs-137 are well known, and all of the pertinent data for each of these isotopes can be found in references [3], [6] and [7] respectively.

Estimate of Radiative Losses for Given Beta Particles

Since ion pair formation is the main concern for this application, energy losses through non-collisional pathways such as Bremsstrahlung must be accounted for. Radiative losses such as Bremsstrahlung represent energy loss mechanism that do not directly form ion pairs and hence detract from the formation of an ion plume. The actual ratio of radiative to collisional energy loss is a complex expression; however the following expression gives an accurate approximation.

$$\frac{(dE/dx)_r}{(dE/dx)_c} \cong \frac{EZ}{700} \qquad (1)$$

where E is energy in units of MeV, and Z is the atomic number of the medium through which the β^- travels. The derivative terms on the left hand side of Eq. (1) represents the ratio of radiative stopping power to the collisional stopping power. Integrating Eq. (1) over all space yields the ratio of total radiative energy loss to total collisional energy loss for a particle of known energy. This approximation is used for each of the isotopes, Co-60 and Cs-137. In order to ensure the estimate is conservative, the maximum β^- energies will be used for E and the highest possible value will be used for Z. Since the

medium of interest is air, which is composed of ~78% nitrogen (Z=7) and 22% oxygen (Z=8), a value of Z=8 will be used.

The results of the calculation for each of the three isotopes are shown in Table 1, and clearly indicate that the amount of energy lost to Bremsstrahlung for each of the three isotopes is negligible. These data are supported by the following conceptual argument: since the kinetic energy of the β^- particle is relatively small, the amount of energy lost in the event of an inelastic collision would likewise be negligibly small. Therefore, it can be assumed that all of a given β^-'s energy is lost to the formation of ions in atmospheric air.

Isotope	Maximum Beta Energy (MeV)	$\frac{(dE/dx)_r}{(dE/dx)_c}$
Kr-85	0.6874	0.7856%
Co-60	0.3182	0.3637%
Cs-137	0.5140	0.5874%

Table 1. Table showing conservative estimates for the total percentage of energy lost to Bremsstrahlung for each of the three isotopes of interest.

Ion Pairs per Beta Particle

The previous section demonstrated that the beta particles from Co-60, Cs-137 and Kr-85 lose all of their energy to the formation of ion-pairs in air. The number of ion pairs corresponding to a typical β^- from each isotope can be calculated. This is an important input parameter for the spatial ion-distribution model, describing the number of ion-pairs expected to be produced per charged particle. It will be assumed that a β^- emitted by a particular isotope has a kinetic energy equal to the average kinetic energy of the spectrum for that isotope. The W-value for air is 33.8 eV/ion-pair [8].

Using this information, the average number of ion pairs created per β^- can be calculated as:

$$\frac{Avg\ eV}{\beta^-\ particle} \div (W-value)\left(\frac{ion\ pairs}{eV}\right) = \frac{ion\ pairs}{\beta^-\ particle} \qquad (2)$$

The information in Table 2 can be used to verify a value for the expected number of ion-pairs created per m³ per second by Kr-85 emissions from reprocessing plants. A study from the WAK reprocessing facility in Germany gives a value of 2.7 mCi/m³s due to Kr-85 emission during reprocessing [4]. Using this data, the number of ion pairs/cm³s can be calculated:

$$\frac{2.7\ \text{mC}i}{\text{m}^3} \times \frac{3.7\times10^{10}\ \text{Bq}}{1000\ \text{mCi}} \times \frac{1^{\beta}/\text{sec}}{1\ \text{Bq}} \times \frac{7443\ \text{ion pairs}}{1\beta}$$

$$= \frac{7.4\times10^{11}\ \text{ion pairs}}{\text{m}^3\text{s}} = \frac{7.4\times10^{5}\ \text{ion pairs}}{\text{cm}^3\text{s}} \qquad (3)$$

Isotope	Avg Beta Energy (eV)	Avg # Ion Pairs/ Beta Particle
Kr-85	251590	~ 7443
Co-60	95770	~ 2833
Cs-137	174320	~ 5157

Table 2. Table showing the expected average number of ion pairs produced in air per beta particle from each of three sources of interest.

The specific production rate of ions due to Kr-85 emissions of the given activity is roughly 7.4 x 10^5 ion-pairs/cm³s. This value can serve as a baseline for experiments where the ion production parameter can be controlled.

A couple of points should be noted about Eq. (3). First, it is assumed that ion pairs are created instantaneously coinciding with the release of a β^-. The β^- has a velocity near the speed of light when released, and its maximum travel length never exceeds three meters as per rule of thumb. Since time = distance/velocity, to a classical approximation, this assumption is valid.

Another more egregious omission is the recombination of ions once they are formed. Models of this process are currently underdeveloped and go beyond the scope of this study, but it is expected that such models will be useful in the future.

Maximum Beta Particle Range in Air

The range of the β^- in air is an important parameter because it represents the distance over which significant ionization is expected to occur. The definition of maximum range of a β^- assumes that the particle traveled in a straight line, although this is rarely ever the case. It has been found that the range is largely a function of the β^- energy, and the density of the medium material, regardless of the material's other properties [8]. Figure 1 illustrates this fact and is used to derive expected values for the range of the β^-'s emitted by each of the above three isotopes. In this case, we will estimate the range x density values for the average energy and the maximum energy of a β^- from each of the three sources. The results can be found in Table 3.

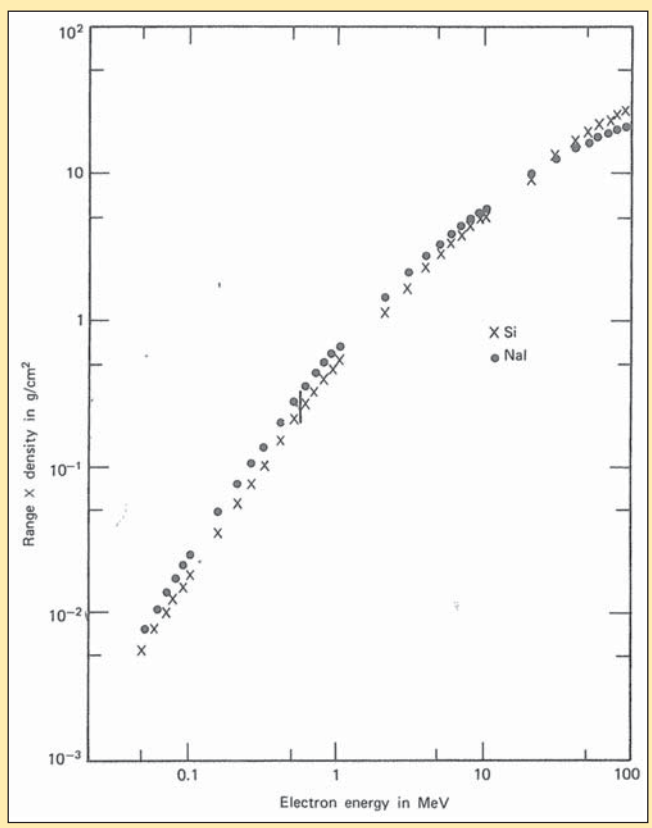

Figure 1. Figure showing the range x density value for several materials as a function of beta particle energy. Notice that the figure shows the trend is relatively constant regardless of which material is considered [8].

Isotope	Max Beta Energy (MeV)	Avg Beta Energy (MeV)	Maximum Estimated Range*Density (g/cm^2)	Average Estimated Range*Density (g/cm^2)	Max Est. Range (cm)	Avg Est. Range (cm)
Kr-85	0.6874	0.25159	0.3	0.06	232.0	46.4
Co-60	0.3182	0.09577	0.1	0.015	77.3	11.6
Cs-137	0.514	0.17432	0.11	0.028	85.1	21.7

Table 3. Estimates of the average and maximum range of the beta particles in air based on the range x density plot (Figure 1). The maximum and average energies of the beta particles were used to determine corresponding "maximum" and "average" range x density values on the chart above. To calculate the range, the range x density values were simply divided by the density of dry air, approximately 0.001293 g/cm^3.

Gamma Ray Interaction in Air

Although Kr-85 is a pure beta emitter, the sources that will likely be used in the lab emit both beta and gamma radiation. For instance, some common lab sources, including Cobalt-60 (Co-60) and Cesium-137 (Cs-137), are dual gamma and β^- emitters. Therefore, it will be useful to know what effect, if any, the gamma radiation will have on ionization.

The probability of a gamma ray interaction in any medium is measured with an attenuation coefficient, μ, which is the probability, per unit path length, that a gamma-ray photon will be removed from a theoretical beam defined by its initial path [8]. The attenuation coefficient is dependent on the energy of the gamma ray, the atomic number of the medium, and the density of the attenuating material. Since the medium of interest in this case is air, we are interested in the attenuation properties of nitrogen and oxygen under reasonable atmospheric conditions. The mass attenuation coefficient (which accounts for density) can be estimated from published graphs and Tables (Graph A, [9] and Table 4).

The density of dry air at standard atmospheric conditions is about 0.001293 g/cm^3 [8]. Using this value for the density, we can calculate the probability per unit path length of an interaction between the gamma ray and the medium. An alternate way to characterize the same property is to calculate the mean free path of the gamma ray in the given medium. The mean free path is defined as the average distance that the gamma ray travels through the medium before any interaction takes place. This value is simply the reciprocal of the attenuation coefficient and is shown in Table 5.

The values for mean free path length for gamma rays from Co-60 and Cs-137 are ~160 m and ~85 m respectively. As rough estimates, even if they are an order of magnitude too high, these values still show that the gamma rays interact far less in air than beta particles do. Hence the ion production rate from gamma rays is expected to be much smaller than that from beta particles. However, in a laboratory setting, the gamma rays are bound to hit other solid materials/equipment and emit secondary energetic electrons which will cause ionization in air like beta particles do. See Eq. (4) for an estimate of ion production rate as a function of distance from a gamma ray source of given activity.

Each of these calculated parameters plays a role in the spatial ionization model. The amount of ions produced per beta particle and the maximum beta particle range help define the magnitude and spatial resolution of the models, respectively. The gamma-ray range in air similarly plays a role in determining the spatial scale of the model. Finally, the calculated absence of radiative losses allows the model to ignore loss terms due to Bremsstrahlung.

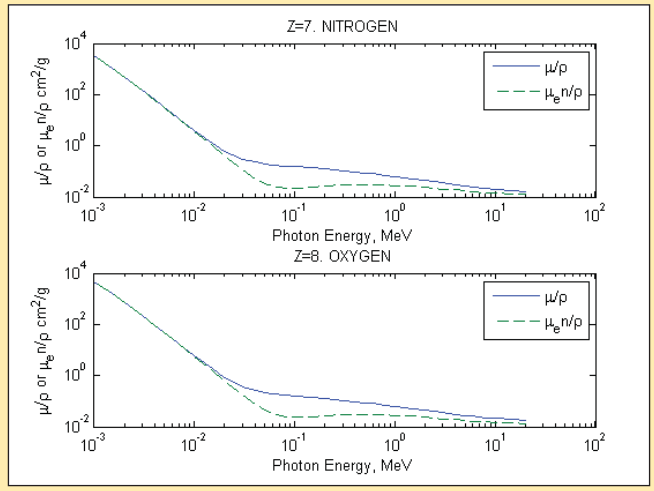

Graph A. Mass attenuation coefficients for nitrogen and oxygen.

Isotope	γ-Energy (MeV)	μ/ρ (cm^2/g) for O	μ/ρ (cm^2/g) for N	Est. μ/ρ (cm^2/g) for Air
Co-60	1.173, 1.332	0.035	0.05	0.0467
Cs-137	0.682	0.09	0.085	0.0861

Table 4. Table showing the estimates for the mass attenuation coefficient for gamma rays in oxygen, nitrogen and air. The oxygen and nitrogen values were estimated using the graphs found in Appendix A. The estimate for air is calculated by the following formula: 0.78 x N-value + 0.22 x O-value. This is intended to compensate for the concentration of nitrogen and oxygen in air.

Isotope	Est. μ/ρ (cm^2/g) for Air	μ (1/cm)	λ (cm)
Co-60	0.0489	6.323E-05	1.582E+04
Cs-137	0.0927	1.20E-04	8.343E+03

Table 5. Table showing the calculated estimates for the mass attenuation coefficient and the mean free path of the gamma rays emitted by the two listed sources.

Spatial Ionization Models for Isotopes of Interest

The information calculated in the above section for Co-60 and Cs-137 was applied in the development of a model to calculate the expected amount of ionization from disk sources of Cs-137 and Co-60 of known activity as a function of distance from the source. These predicted values will then be compared to any measured changes in cross section to greater understand the relationship between ion concentration and changes in radar cross section. Co-60 and Cs-137 were considered for this ion model because these isotopes will most likely be used for laboratory tests of MMW technology. Furthermore, the results of these models could easily be extended to Kr-85 sources, since the principles used to derive the parameters in the calculations section do not differ for different isotopes.

Results and Discussion

Since ionization is, by far, the most prevalent pathway by which gamma ray energy can lose energy in air, the measure of charge/unit mass (gamma source exposure rate) can easily be converted to ion-pairs/unit mass. The exposure rate equation is based on the assumption that the volume of interest is large compared to the size of the source (i.e., spherical geometry is applicable). Since the mean free path of the high energy gamma rays of interest is on the order of tens of meters in air, and since most lab sources tend to be small disk sources, this assumption is upheld quite well. The equation for calculating exposure rate from activity is given by Knoll [8] as:

$$X = \Gamma \frac{A}{d^2} \tag{4}$$

where,

X = exposure rate (R/hr)

Γ = the exposure rate constant (R x cm²)/(hr x mCi)

A = Activity (mCi)

d = straight-line distance from source to point of interest (cm).

Eq. (4) shows that exposure rate can be calculated as a function of distance if the activity and the exposure rate constant are known for the isotopes of interest. Exposure rate constants can be found in a number of radiological health resources [10], while the activity must be a given parameter. The parameters of interest for Co-60 and Cs-137 are given in Table 6.

Isotope	Exposure Rate Constant (R*cm²)/(hr*mCi)	Activity (mCi)
Cs-137	3.3	0.4
Co-60	13.2	0.95

Table 6. Exposure rate constants and activities for Cs-137 and Co-60. The exposure rate constants were looked up on page 59 of reference 8. The activities of the sources were specified by the designers of the experiment.

The conversion between Roentgen and ion-pairs per mass is: 1R = 2.08 x 10^9 ion-pairs/0.001293 g air (1 cm³ at standard temperature and pressure (STP)) [8]. Therefore, if it is assumed that the medium is at STP, the value for exposure rate can be converted to ion-pairs/cm³/s; which is the parameter of interest.

Carrying out the calculation for Co-60 and Cs-137 and then converting the answer to ion-pairs/cm³/s yields:

$$\dot{X} = 13.2\frac{0.4}{d^2} = \frac{12.6}{d^2}\,\frac{R}{hr} * \frac{1\,hr}{3600\,s} = 0.0035\frac{R}{s} * \frac{2.08 \times 10^9 \text{ ion pairs/cm}^3}{1R} \Longrightarrow \frac{7.28 \times 10^6}{d^2}\,\frac{\text{ion pairs}}{\text{cm}^3\text{s}} \tag{5}$$

for Co-60 and

$$\dot{X} = 3.3\frac{0.4}{d^2} = \frac{1.32}{d^2}\,\frac{R}{hr} * \frac{1\,hr}{3600\,s} = 0.000367\frac{R}{s} * \frac{2.08 \times 10^9 \text{ ion pairs/cm}^3}{1R} \Longrightarrow \frac{7.63 \times 10^5}{d^2}\,\frac{\text{ion pairs}}{\text{cm}^3\text{s}} \tag{6}$$

for Cs-137.

Therefore, given the distance in centimeters, the number of ion pairs produced per cm³ of air as a result of gamma ray radiation is 7.28 x $10^6/d^2$ ion pairs/cm³/s for Co-60 and 7.63 x $10^5/d^2$ ion pairs/cm³/s for Cs-137. At a sample distance from the source of 10 cm, these equations yield 7.28 x 10^4 ion pairs/cm³/s for Co-60 and 7.63 x 10^3 ion pairs/cm³/s for Cs-137.

Unlike the gamma ray case, no convenient equation exists to calculate the amount of ionization as a function of the spatial distribution of the beta particles. In order to estimate the amount of ion-pair production as a function of spatial distribution, a simple spatial model will be derived based on the following assumptions.

1. Although beta particles are emitted with a spectrum of possible energies, it will be assumed that each beta particle emitted by the source leaves with the average energy for that particular spectrum (i.e., 95.77 keV for Co-60 and 174.32 keV for Cs-137).
2. Since the path of beta particles is erratic in air, the overall motion of any given beta particle will be characterized as random. It follows that the ion pairs due to beta radiation follows a Gaussian spatial distribution.
3. From the central limit theorem, it can be shown that 99.7% of the expected values will reside within three standard deviations of the mean for a normal distribution. In this case, the mean value is zero (in other words, the average value of the distance traveled is zero, since the emission of beta particles from the source is assumed to be spherically symmetric). Therefore, it will be stated that three standard deviations will correspond to the maximum range of a beta particle in air.
4. The magnitude of the distribution can be calculated in the following manner. Given the average number of ion pairs produced per beta particle as calculated above and the number of beta particles emitted per unit time which can be estimated by the activity of the source, the Cs-137 source is expected to emit 0.4 x 3.7 x 10^7 = 1.48 x 10^7 beta particles/second, while the Co-60 source is expected to emit 0.95 x 3.7 x 10^7 = 3.52 x 10^7 beta particles/second. Therefore, the number of ion pairs produced per second due to beta radiation is:

   1.48 x 10^7 x 2 833 = 4.19 x 10^{10} ip/s for Co-60,

   and 3.52 x 10^7 x 5 157 = 1.81 x 10^{11} ip/s for Cs-137.

   The general form for a Gaussian distribution [11] is given by:

$$f(x) = \frac{A}{\sigma\sqrt{2\pi}} \exp\left(-\frac{x^2}{2\sigma^2}\right) \tag{7}$$

where A is the magnitude of the distribution, σ is the standard deviation, and x is the single spatial dimension considered. Calculating A and σ as described above, we are left with the parameters given in Table 7 for Co-60 and Cs-137.

Isotope	A (ip/s)	Max Range (cm) (from Table 3)	σ (cm)
Cs-137	1.18E+11	77.3	28.3
Co-60	4.19E+10	85.1	25

Table 7. Parameters A and σ for Cs-137 and Co-60 as calculated for the spatial ion model above.

It does not matter whether an ion pair was created indirectly by gamma ray interactions or by beta particle interactions. The total number of ion pairs at any given distance is expected to be the sum of the ion pairs created by gamma radiation and beta radiation. Thus, combining all of the information above, the spatially-dependent functions of ion density for each isotope is:

$$f(x[\text{cm}]) = \frac{A}{\sigma\sqrt{2\pi}} \exp\left(-\frac{x^2}{2\sigma^2}\right) + \frac{7.08 \times 10^6}{x^2} \tag{8}$$

for Co-60, where

$A = 4.19 \times 10^{10}$ ip/s;

$\sigma = 25$ cm;

x = distance from source (cm);

and

$$f(x[cm]) = \frac{A}{\sigma\sqrt{2\pi}} \exp\left(-\frac{x^2}{2\sigma^2}\right) + \frac{7.63 \times 10^5}{x^2}$$; where

$A = 1.81 \times 10^{11}$ ip/s;

$\sigma = 28.33$ cm;

x = distance from source (cm);

for Cs-137.

Conclusion

Figures 2 and 3 show the results of these models plotted in two dimensions from which we can conclude that the contribution of ion pairs due to gamma radiation is negligible compared to the amount of ion pairs produced by beta radiation. This matches the prediction made above.

One of the shortcomings of this model is that it does not take into account recombination. The simplest models for recombination are often shown in differential form such that: $\frac{dn}{dt} = -\alpha * n^2$ where n(t) is the concentration of ions and alpha is a recombination coefficient [5]. However, this model is not accurate in this case because the mechanisms for recombination in the atmosphere are far more complex than this model suggests. Also, values for α are not accurately known for situations where ion concentrations are higher than the general background level. Since recombination is not considered in the above model, the density of ions predicted by the model may be somewhat higher than what is observed. More research is needed to better understand the role of recombination in high-ion density atmospheric situations.

Also, notice that the ion-pair densities predicted by the model are given in ip/cm³s. The time dependence is a consequence of the activity of the sources. In a previous model it has been shown that the ion concentration tends to approach the value predicted by the time dependent model in a relatively short time frame. This indicates that after several milliseconds, the densities predicted by the model tend to be time independent. This is largely due to diffusion and recombination of ions.

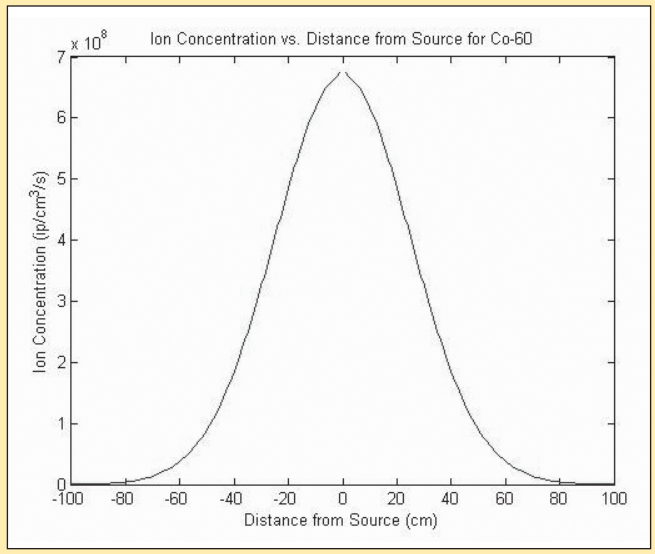

Figure 2. A figure showing the spatial distribution of ion pairs from the decay of a 0.95 mCi disk source of Co-60.

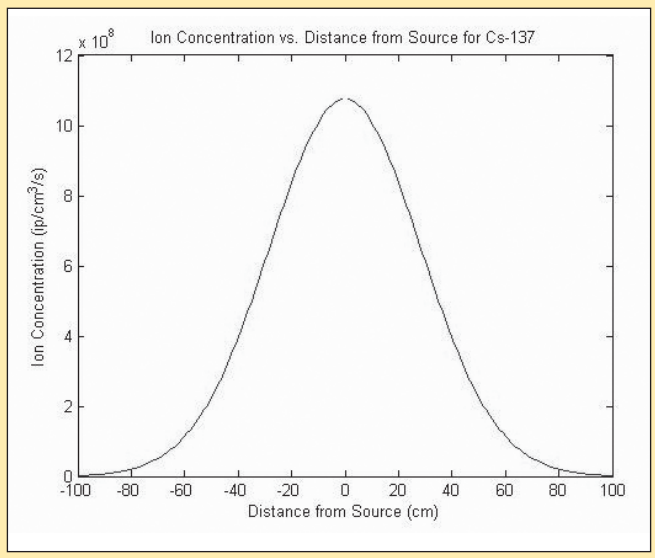

Figure 3. A figure showing the spatial distribution of ion pairs from the decay of a 0.4 mCi disk source of Cs-137.

Due to their ready availability, Co-60 and Cs-137 were identified as the most obvious choices for laboratory sources to be used to test and calibrate the MMW detection technology. Parameters such as the range of beta particles in air, the range of gamma rays in air, and the number of ion-pairs expected to be produced by each type of radiation were calculated. These parameters were then incorporated into a spatial ion model based on a Gaussian spatial distribution. The results of these models will be used as a starting point against which the detection data from MMW tests in the laboratory can be

checked. Currently, this model is based on generalized assumptions, and will be refined upon collecting data using the MMW detection system.

Acknowledgements

This research was conducted at Argonne National Laboratory. I would like to take this opportunity to thank my mentor Nachappa Gopalsami. He has given me a great introduction to laboratory work and research. Also, he has inspired me not only to continue along my academic path, but to broaden my horizons, and has introduced me to new areas of study which I plan to pursue. I would also like to thank H.T. Chien for his mentorship and guidance in the laboratory. Finally, I would like to thank the Department of Energy, Office of Science for their sponsorship of the SULI Program and for affording me the opportunity to participate in such a fulfilling program.

References

[1] Z. Mian and A.H. Nayyar, "An Initial Analysis of Kr-85 Production and Dispersion from Reprocessing in India and Pakistan," Science and Global Security, vol.10, Number 3. pp. 151–179, September 2002.

[2] M.B. Kalinowski, H. Daerr and M. Kohler, "Measurements of Krypton-85 to Detect Clandestine Plutonium Production," *INESAP Bulletin 27*, January 2008, www.inesap.org/bulletin27/art02.htm.

[3] H. Sievers, Nuclear Data Sheets 62,271, 1991, http://www.nndc.bnl.gov/nudat2/decaysearchdirect.jsp?nuc=85KR&unc=nds.

[4] M.B. Kalinowski, H. Sartorius, S. Uhl and W. Wolfgang, "Conclusions on Plutonium Separation from Atmospheric Kr-85 Measured at Various Distances from the Karlsruhe Reprocessing Plant," *Journal of Environmental Radioactivity*, vol. 73, Issue 2, pp. 203–222, September 2003.

[5] K.A. Boyarchuk, E.N. Kononov and G.A. Lyakhov, "Radar Observation of Regions of Local Ionization in the Lower Layers of the Atmosphere," Technical Physics Letters, vol.19, Issue 3, pp. 184–186, March 1993.

[6] J.K. Tuli, Nuclear Data Sheets (100,347), 2003, June 2008, http://www.nndc.bnl.gov/nudat2/decaysearchdirect.jsp?nuc=60CO&unc=nds.

[7] E. Browne and J.K. Tuli, Nuclear Data Sheets 108, 2173, 2007, http://www.nndc.bnl.gov/nudat2/decaysearchdirect.jsp?nuc=137CS&unc=nds.

[8] G.F. Knoll, "Radiation Detection and Measurement," 3rd ed., New York: John Wiley & Sons Inc., 2000.

[9] J.H. Hubbel and S.M. Seltzer. "Tables of X-Ray Mass Attenuation Coefficients and Mass Energy-Absorption Coefficients," June 2008, http://physics.nist.gov/PhysRefData/XrayMassCoef/cover.html.

[10] B. Shleien, *The Health Physics and Radiological Health Handbook*, Olney, MD: Nucleon Lectern Associates, 1984.

[11] R. Haberman, "Applied Partial Differential Equations with Fourier Series and Boundary Value Problems," 4th ed., Upper Saddle River, New Jersey, Pearson Prentice Hall, 2004.